Vol 18 No 6, June 2009
1674-1056/2009/18(06)/2264-07

Chinese Physics B

© 2009 Chin. Phys. Soc.
and IOP Publishing Ltd

Appearance of metallic features in small tungsten clusters*

Lei Xue-Ling(雷雪玲)[a)], Wang Xian-Ming(王先明)[a)],
Zhu Heng-Jiang(祝恒江)[a)†], and Luo You-Hua(罗有华)[b)]

[a)] *School of Maths-Physics and Information Sciences, Xinjiang Normal University, Urumqi* 830054, *China*
[b)] *Department of Physics, East China University of Science and Technology, Shanghai* 200237, *China*

(Received 1 August 2008; revised manuscript received 17 November 2008)

The structures and properties of W_n (n = 2–14) clusters were studied by using the density functional theory (DFT) at LSDA level. The most stable structures of W_n (n = 2–14) clusters with global minimum were determined. The average binding energy (E_b), the first and second difference of total energy (ΔE, $\Delta_2 E$), the vertical detachment energy (VDE), and the HOMO-LUMO gap versus the size were also discussed. The abrupt decrease of VDE and HOMO-LUMO gap at size n = 8 and 10 implied that tungsten clusters of W_8 and W_{10} appeared to have metallic features. These changes were also accompanied by the delocalization of electron charge density and the strong hybridization between 5d and 6s orbits in W_8 and W_{10} clusters. Our results are in good agreement with the available experimental data.

Keywords: W_n clusters, density functional theory, lowest-energy structures, metallic features
PACC: 3640, 3640B, 7115M

1. Introduction

It is well known that the geometries and electronic properties of clusters are very different from their bulks.[1−3] For example, clusters of metallic elements exhibit fivefold symmetry and icosahedral growth, which is nonexistent in crystals.[4] The building block of silicon clusters is a tricapped trigonal prism (TTP), which is completely different from the bulk diamond structure.[5,6] Some of the most stable carbon clusters have the famous fullerene geometry while bulk carbon exists in either planar or tetrahedral structures.[7] These interesting phenomena in nano-dimensions raise a fundamental question: what is the critical cluster size at which electronic and geometric structures converge to the bulk properties?[8]

Tungsten is an important rare metal with characteristics such as a high melting point (3380 °C), high hardness and extraordinary chemical stability. It is widely used in modern technology in pure metal and alloy. As far as we know, small tungsten clusters have been studied in many experiments and theories.[9−18] These works included thermionic electron emission of small tungsten cluster anions on the milliseconds time scale,[10] photoelectron imaging spectroscopy of small tungsten clusters,[11] optical and Raman spectroscopy of mass-selected tungsten dimers in argon matrices,[12] and so on. Tungsten dimer and trimer had been studied by using density functional theory (DFT).[13] Zhang *et al*[14] studied small W_n (n = 2–4) clusters in their neutral and anionic states by using DFT at B3LYP/ LanL2DZ level, predicting that both W_3 and W_4 were spin triplet and the ground state of W_4 was a plane rhombus with D_{2h} symmetry. Yamaguchi *et al*[15] studied geometries of anionic, neutral, and cationic small tungsten clusters W_n (n = 3–6) by using DFT at B3LYP/ LanL2DZ level, finding that W_3 and W_6 were spin triplet, and W_4 and W_5 were spin singlet. Oh *et al*[16] studied structural evolution of W nano-clusters with the increase of cluster size by x-ray diffraction (XRD) patterns, finding that the structure changed from amorphous to face-centered-cubic (fcc) to body-centered-cubic (bcc) with the increase of the average cluster size. Lee *et al*[17] recorded photoelectron spectra of W_n^- (n = 20–90) by using a magnetic bottle-type photoelectron spectrometer, estimating that metallic properties might begin at the cluster size n = 10. Lin *et al*[18] studied the evolution from nonmetallic to metallic features of W clusters, predicting that the transition from semiconductor-like to metallicity might take place around the size n = 8.

Due to the mutual contradiction of the above con-

*Project supported by the Excellent Young Teachers' Foundation of Xinjiang Normal University (Grant No XJNU0730) and the Prior Developing Subject' Foundation of Xinjiang Normal University.
†Corresponding author. E-mail: zhj@xjnu.edu.cn

clusions of experiments and theories, we carried out a systematic study of W_n (n = 2–14) clusters from first principles molecular orbital calculations, analyzing the evolution from nonmetallic to metallic features of tungsten clusters. This work may facilitate the understanding of geometric structures, electronic shell structures and the bonding nature for other clusters in the future.

2. Computation methods

In this paper, all the calculations for W_n (n = 2–14) clusters are performed with the LSDA (SVWN) hybrid density functional method and the LanL2DZ basis set[19] in the Gaussian 03[20] package. In order to test the reliability of the LSDA/LanL2DZ scheme for the description of W_n clusters, some properties of the W dimer are calculated by using five different exchange-correlation functional methods at the same LanL2DZ basis set. Among these methods, the calculated vibrational frequencies, electron affinities, and ionization potential for W dimer by LSDA/LanL2DZ scheme are in good agreement with the available experimental data (Table 1),[12,9,21] so it is reasonable to use the same method throughout the whole calculations. The calculation convergence criterion for the RMS force criterion is set to 3×10^{-4} a.u. The stabilities of W_n clusters are examined by the vibrational frequencies calculation. For each of the clusters, all computed frequencies are confirmed as real. Moreover, spin unrestricted calculations are performed for all allowable spin multiplicities.

Table 1. The total energy (E_t), bond length (R_e), vibrational frequencies (ω_e), binding energy per atom (E_b), electron affinity (EA), and ionization potential (IP) of W_2 at DFT/B3LYP, B3PW91, LSDA, MPW1PW91, PBE1PBE /LanL2DZ level.

cluster	E_t/a.u.	R_e/nm	ω_e/cm^{-1}	E_b/eV	EA/eV	IP/eV
W_2 B3LYP	–135.40113823	0.2039	410.558	4.548	0.899	6.668
B3PW91	–135.46371288	0.2031	418.428	4.936	1.037	6.700
LSDA	–135.73994683	0.2037	409.925	6.481	1.650	7.665
MPW1PW91	–135.40635738	0.2025	423.608	4.796	1.004	6.612
PBE1PBE	–135.33084882	0.2025	423.808	4.831	0.977	6.588
Exp.			336.8[a]		1.46[b]	5.0[c]±1[d]

[a]Ref.[12], [b]Ref.[9], [c]Ref.[9], estimated from Fig.3., [d]Ref.[21], estimated value.

For each initial structure, we research it extensively in three ways: (i) Consider all of the possible structures reported in the previous papers. (ii) Design different dimensional patterns for W_n clusters; e.g., for W_3, the linear structure, the planar equilateral triangle or isosceles triangle or unsymmetric triangle are all designed. (iii) Adding a tungsten atom to the different places of the W_n clusters which have been optimized, we can obtain W_{n+1} clusters.

3. Results and discussion

3.1. Geometries of W_n (n = 2–14) clusters

The lowest energy structures, some meta-stable isomers, and symmetries for W_n (n = 2–14) clusters are presented in Fig.1. According to the calculations, the spin multiplicity of ground states for W_n (n = 2–14) clusters are all singlet except W_3. For W_3, the ground state 3a(3) is spin triplet and has an equilateral triangle geometry with D_{3h} symmetry, consistent with the previous theoretical results.[13−15,22] However, the spin singlet state 3a(1) has an isosceles triangle geometry with C_{2v} symmetry, only 0.123 eV higher than the spin triplet, which is a competitive candidate for the ground state. There is a negative vibrational frequency for the 3b(1) structure, so it is a saddle point of the potential energy surface. For W_4, the ground state 4a(1) has a tetrahedral geometry with spin singlet state, while the other isomer 4b(1) with a plane rhombus is 0.225 eV higher than 4a(1). This result is in agreement with the result obtained by Lin and Cai,[18,22] different from Zhang and Yamaguchi.[14,15] For W_5, our result is consistent with

the result obtained by Yamaguchi *et al.*[15] For W_6, we find that the lowest energy state is spin singlet, and it has a twisted octahedron or twisted trigonal prism geometry with C_1 symmetry. This result is inconsistent with the result by Yamaguchi *et al.*[15] For W_7–W_{14}, our results are different from Lin *et al*,[18] who predicted that the ground state of W_7 is a decahedron geometry. For $n > 7$, the geometry of W_n can be taken as growing on the basis of decahedron geometry by adding W atom continually. In our calculations, the W_7 structure is a bicapped five-sided rings. For $n > 7$, the growth patterns are cage or prolate, containing small unit. For example, $n = 8$–10, the geometries include the unit of W_8; $n = 11$–14, the geometries include the unit of W_7. Especially, the W_{12} can be understood as the immediate consequence of nestification in which double W_7 share two common W atoms.

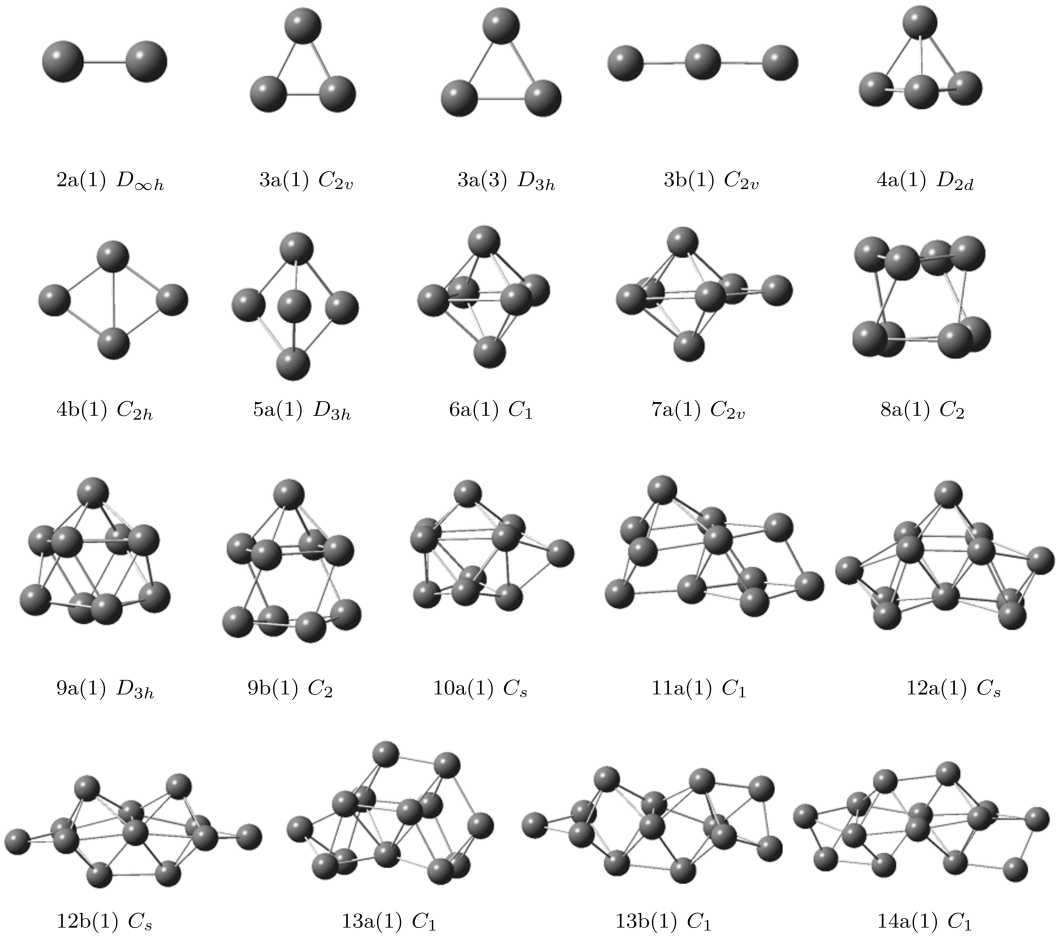


Fig.1. The geometries and symmetries of W_n ($n = 2$–14) clusters.

3.2. Relative stabilities of W_n ($n = 2 - 14$) clusters

The relative stabilities of the different sized clusters can be predicted by calculating the average binding energy, the first-order difference and the second-order difference of total energy which can be defined by the following formulas:

$$E_b(n) = \frac{nE(W) - E(W_n)}{n}, \tag{1}$$

$$\Delta E\left(W_n\right) = E\left(W_{n-1}\right) + E\left(W\right) - E\left(W_n\right), \tag{2}$$

$$\Delta_2 E\left(W_n\right) = E\left(W_{n+1}\right) + E\left(W_{n-1}\right) - 2E\left(W_n\right), \tag{3}$$

where E is the total energy of the system. The average binding energy (E_b), the first-order difference (ΔE) and the second-order difference of total energy

($\Delta_2 E$) for ground states of W_n clusters are plotted in Figs.2–4, respectively. E_b refers to the binding energy per atom, ΔE refers to the capacity of removing a W atom from tungsten clusters, $\Delta_2 E$ is a sensitive quantity characterizing relative stability of atomic clusters, which can be compared directly with the relative mass spectrum abundance of clusters in experiments. From Fig.2, it can be seen that the average binding energy increases monotonically with cluster size. Thus, the clusters can continue to gain energy during the growing process. Moreover, the curve reveals that the local peak appears at $n = 13$, indicating that W_{13} is more stable than its neighbors, which can also be obtained from Figs.3 and 4. From Fig.3 we can see that the local peaks are found at $n = 2$, 6, 9, and 13 while the local minima are found at $n = 3$, 7 and 11. From Fig.4 we can see that the local peaks are found at $n = 2$, 6, 9, and 13 while the local minima are found at $n = 4$, 7 and 11. These results indicate that W_6, W_9, and W_{13} are more stable than their neighbors while W_7 and W_{11} are less stable than their neighbors. W_7 is less stable perhaps because it is a turning point from nonmetallic to metallic features of tungsten clusters. W_{11} is less stable perhaps because its geometry experiences a transition from cage to prolate. The magic numbers of tungsten clusters are inconsistent with the results obtained by Lin *et al.*[18] This is because the structures are not the global minimum, but the local minimum growing on the basis of decahedron geometry of W_7 for $n > 7$.

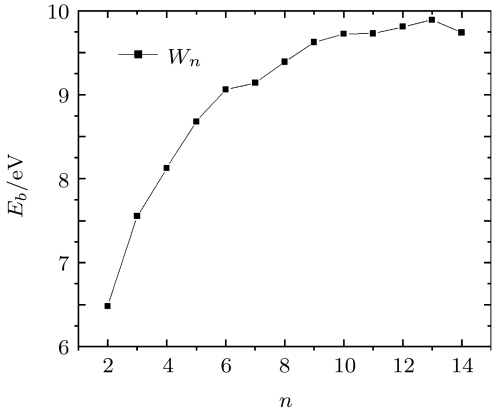


Fig.2. The E_b/atom versus n.

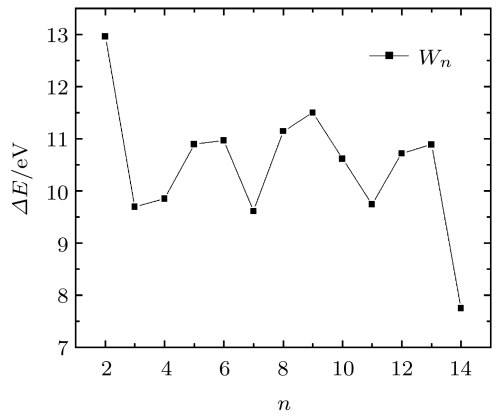


Fig.3. The ΔE versus n.

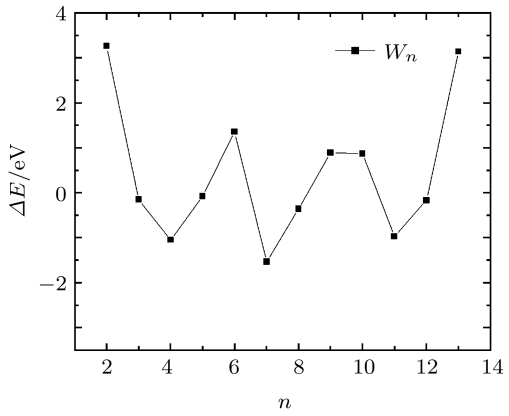


Fig.4. The $\Delta_2 E$ versus n.

3.3. Analysis of metallic features

In order to have a better perspective on the metallic features of tungsten clusters, we calculate the vertical ionization potential (difference between the energies of the cation and the neutral at the neutral geometry, VIP) and energy gap (difference between the energies of highest occupied molecular orbit (HOMO) and lowest unoccupied molecular orbit (LUMO), the Gap). The VIP and the Gap versus the size of cluster are shown in Figs.5 and 6, respectively.

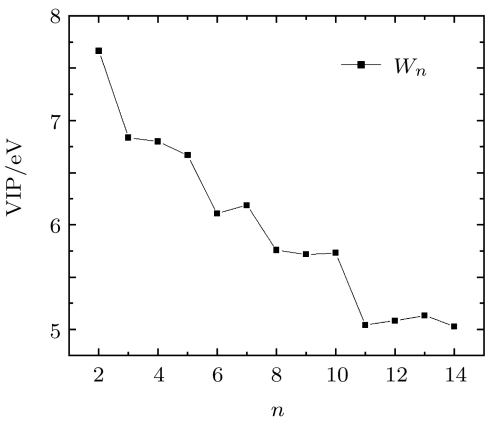


Fig.5. The VIP versus n.

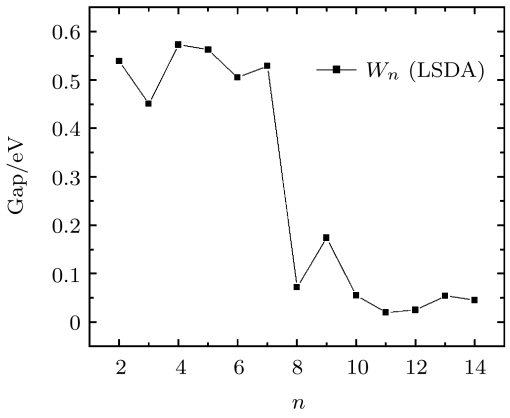


Fig.6. The Gap versus n (LSDA).

Figure 5 presents the VIP versus size. The VIP decreases monotonically with the cluster size, which is the characteristic of transition from nonmetal to metallic behavior.[8] This trend can also be seen in Fig.6.

Figure 6 presents the energy gap (Gap) between HOMO and LUMO for W_n (n = 2–14) clusters. From Fig.6 we can see that the energy gap decreases with the cluster size. Finally, it no longer has the separate-molecular-behavior characteristic, but shows the bulk phase energy level. Generally, a cluster with a larger (non-zero) HOMO-LUMO gap exhibits semiconducting behavior while a cluster with smaller (nearly vanishing) HOMO-LUMO gap exhibits metallic behavior. As can be seen from Fig.6, the HOMO-LUMO gap is relatively large (0.451 eV–0.573 eV) for n = 2–7, suggesting the nonmetallic features in these clusters. For n = 8, the HOMO-LUMO gap decreases sharply, and becomes particularly small (0.072 eV), indicating that the metallic properties may appear at this cluster size. It should be noticed that a metallic property begins from small clusters such as $n = 10$[23,24] in many metals. For n = 8–10, the HOMO-LUMO gap displays oscillating tendency. The gap is only 0.055 eV at n = 10, indicating that W_{10} also appears metallic properties. For n = 11–14, the HOMO-LUMO gap displays a slight decreasing tendency, and is relatively small (below 0.054 eV). Therefore, the appearance of metallic features of tungsten clusters can be set at n = 10. This result is in good agreement with the available experimental data.[17]

In order to test the reliability of the energy gap of W_n (n = 2–14) clusters, we also calculate it at B3LYP/LanL2DZ level. The results are shown in Fig.7. We find that the two calculated energy gaps all decrease with cluster size. For W_n (n = 2–14) clusters, the variations of the energy gaps obtained by using LSDA and B3LYP procedures agree well with each other.

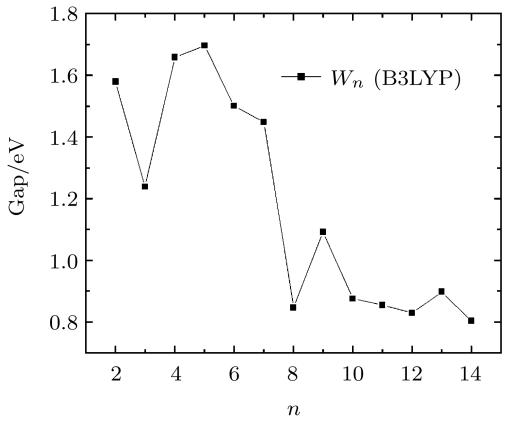
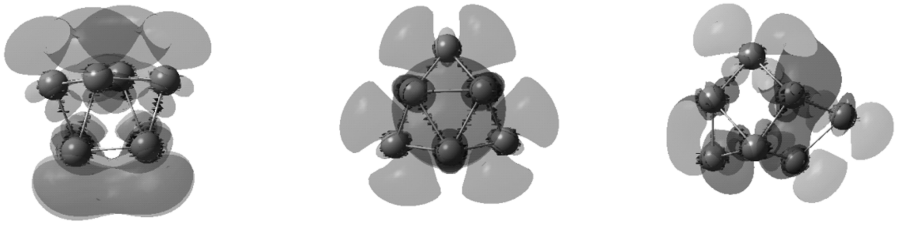


Fig.7. The Gap versus n (B3LYP).

In addition, to further confirm the results, the HOMO orbits of W_8, W_9 and W_{10} are calculated, as shown in Fig.8. The HOMO orbits in W_8 and W_{10} are contributed by W atoms, the electron distribution is delocalized, as expected for metallic bonding. Yet in W_9 cluster, the electrons are localized considerably.



n = 8 HOMO-56 n = 9 HOMO-63 n = 10 HOMO-70

Fig.8. The part HOMO (n = 8, 9, 10).

Moreover, in order to gain a more profound insight into the metallic evolution of tungsten clusters, we study the *s*-*d* hybridization of W atoms. The average electronic number of $6s$ and $5d$ of W atoms is presented in Table 2. The electronic number of $6s$ appears oscillation at $n = 2$–4, depending on the transition from noncovalent bond to covalent bond. The electronic number of $6s$ orbit is less than 2, decreasing gradually at $n > 4$. While the electronic numbers of $5d$ orbit is more than 4, increasing gradually at $n > 4$. It is well known that the outer valence electron configuration of free W atom is $5d^4 6s^2$, and there is a strong hybridization occurs between $5d$ and $6s$ of the W atom at $n > 4$. Especially at $n = 10$, the electronic number of $6s$ orbit is minimum (0.56 e), so the hybridization is more significant, accounting as the transition from covalent bond to metallic bond at the size $n = 10$. These results further confirm that the evolution of the W_n cluster from the nonmetallic to metallic features takes place at W_{10}.

Table 2. The average electronic number of $6s$ and $5d$ (W).

cluster size	$6s$	$5d$
2	1.00	5.01
3	1.13	4.71
4	0.96	4.66
5	0.86	4.75
6	0.73	4.90
7	0.71	4.92
8	0.68	4.95
9	0.62	4.97
10	0.56	4.99
11	0.96	5.02
12	0.92	5.06
13	0.60	4.96
14	0.63	4.96

4. Conclusion

In summary, we have studied the structures and electronic properties of W_n ($n = 2$–14) clusters from first-principles, including their lowest-energy structures, relative stabilities and metallic features. We found that: (i) W_6, W_9, and W_{13} are the magic clusters with higher stabilities while W_7 and W_{11} were less stable. (ii) The tendency of HOMO-LUMO gap change agrees well with those obtained from LSDA and B3LYP level. For $n = 8$ and $n \geq 10$, the HOMO-LUMO gap is obviously small. So the appearance of metallic features of tungsten clusters could be set at $n = 10$. (iii) The atomic orbits exhibit hybridizations with the increase of cluster size, e.g., the hybridizations between the $6s$ orbit and $5d$ orbit lead to covalent bond nature in the clusters for $n < 10$. Further hybridizations of atomic orbits might lead to both the overlaps of the $6s$ orbit and $5d$ orbit and the formation of the metallic bond. The hybridizations of atomic orbits result in the transition from covalent bonding to metallic bonding for $n \geq 10$.

References

[1] Lei X L, Zhu H J, Wang X M and Luo Y H 2008 *Chin. Phys.* B **17** 3687

[2] Lei X L, Wang Q L, Yan Y L, Zhao W J, Yang Z and Luo Y H 2007 *Acta Phys. Sin.* **56** 4484 (in Chinese)

[3] Lei X L, Zhu H J, Ge G X, Wang X M and Luo Y H 2008 *Acta Phys. Sin.* **57** 5491 (in Chinese)

[4] Martin T P, Bergmann T, Göhlich H and Lange T 1990 *Chem. Phys. Lett.* **172** 209

[5] Raghavachari K and Rohlfing C M 1991 *J. Chem. Phys.* **94** 3670

[6] Müller J, Liu B, Shvartsburg A A, Ogut S, Chelikowsky J R, Michael Siu K W, Ho K M and Gantefor G 2000 *Phys. Rev. Lett.* **85** 1666

[7] Kroto H W, Heath J R, O'Brien S C, Curl R F and Smalley R E 1985 *Nature* **318** 162

[8] Sun Q, Rao B K, Jena P, Stolcic D, Kim Y D, Gantefor G and Castleman Jr. A W 2004 *J. Chem. Phys.* **121** 9417

[9] Weidele H, Kreisle D, Recknagel E, Schulze Icking-Konert G, Handschuh H, Ganteför G and Eberhardt W 1995 *Chem. Phys. Lett.* **237** 425

[10] Weidele H, Kreisle D, Recknagel E, Becker S, Kluge H J, Lindinger M, Schweikhard L, Walther C and Ziegler J 1999 *J. Chem. Phys.* **110** 8754

[11] Baguenard B, Pinaré J C, Bordas C and Broyer M 2001 *Phys. Rev.* A **63** 023204

[12] Hu Z D, Dong J G, Lombardi J R and Lindsay D M 1992 *J. Chem. Phys.* **97** 8811

[13] Wu Z J 2003 *Chem. Phys. Lett.* **370** 510

[14] Zhang X R, Ding X L, Dai B and Yang J L 2005 *J. Mol. Struct.*: *Theochem* **757** 113

[15] Yamaguchi W and Murakami J 2005 *Chem. Phys.* **316** 45

[16] Oh S J, Huh S H, Kim H K, Park J W and Lee G H 1999 *J. Chem. Phys.* **111** 7402

[17] Lee G H, Huh S H, Park Y C, Hayakawa F, Negishi Y, Nakajima A and Kaya K 1999 *Chem. Phys. Lett.* **299** 309

[18] Lin Q B, Li R Q, Wen Y H and Zhu Z Z 2008 *Acta. Phys. Sin.* **57** 181 (in Chinese)

[19] Hay P J and Wadt W R 1985 *J. Chem. Phys.* **82** 299

[20] Frisch M J, Trucks G W, Schlegel H B, Scuseria G E, Robb M A, Cheeseman J R, Montgomery J A Jr, Vreven T, Kudin K N, Burant J C, Millam J M, Iyengar S S, Tomasi J, Barone V, Mennucci B, Cossi M, Scalmani G, Rega N, Petersson G A, Nakatsuji H, Hada M, Ehara M, Toyota K, Fukuda R, Hasegawa J, Ishida M, Nakajima T, Honda Y, Kitao O, Nakai H, Klene M, Li X, Knox J E, Hratchian H P, Cross J B, Adamo C, Jaramillo J, Gomperts R, Stratmann R E, Yazyev O, Austin A J, Cammi R, Pomelli C, Ochterski J W, Ayala P Y, Morokuma K, Voth G.A, Salvador P, Dannenberg J J, Zakrzewski V G, Dapprich S, Daniels A D, Strain M C, Farkas O, Malick D K, Rabuck A D, Raghavachari K, Foresman J B, Ortiz J V, Cui Q, Baboul A G, Clifford S, Cioslowski J, Stefanov B B, Liu G, Liashenko A, Piskorz P, Komaromi I, Martin R L, Fox D J, Keith T, Al-Laham M A, Peng C Y, Nanayakkara A, Challacombe M, Gill P M W, Johnson B, Chen W, Wong M W, Gonzalez C and Pople J A 2004 *Gaussian 03*, Gaussian Inc., Wallingford CT

[21] Morse M D 1986 *Chem. Rev.* **86** 1049

[22] Cai S, Neyman K M, Hu A and Rösch N 2000 *J. Phys. Chem.* B **104** 11506

[23] Iseda M, Nishio T, Han S Y, Yoshida H, Terasaki A and Kondow T 1997 *J. Chem. Phys.* **106** 2182

[24] Yoshida H, Terasaki A, Kobayashi K, Tsukuda M and Kondow T 1995 *J. Chem. Phys.* **102** 5960